Particle-Size Distribution As Indicator for Fecal Bacteria Contamination of Drinking Water from Karst Springs

MICHIEL PRONK,[†]
NICO GOLDSCHEIDER,*[,†] AND
JAKOB ZOPFI[‡]

Center of Hydrogeology, and Laboratory of Microbiology, Institute of Biology, University of Neuchâtel, Emile-Argand 11, 2009 Neuchâtel, Switzerland

Received August 08, 2007. Revised manuscript received September 28, 2007. Accepted October 02, 2007.

Continuous monitoring of particle-size distribution (PSD), total organic carbon (TOC), turbidity, discharge and physicochemical parameters, together with analyses of fecal indicator bacteria, particularly *Escherichia coli*, made it possible to better understand the processes governing pathogen transport in karst groundwater and to establish PSD as indicator for possible microbial contamination of drinking water from karst springs. In the study area near Yverdon-les-Bains, Switzerland, tracer tests proved connection between a sinking stream draining agricultural land and several springs, 4.8–6.3 km away. Tracing and monitoring results demonstrate that (i) suspended particles (turbidity) in the spring water either originate from remobilization of sediments inside the aquifer (autochthonous) or from the sinking stream and land surface (allochthonous); (ii) allochthonous turbidity coincides with increased *E. coli* and TOC levels; (iii) PSD makes it possible to distinguish the two types of turbidity; (iv) a relative increase of finer particles (0.9–10 μm) indicates allochthonous turbidity and thus possible fecal contamination. The method permits to optimize water treatment and identify periods when the spring water must be rejected. Findings from other test sites confirm the feasibility of this approach.

Introduction

Microbial pathogens in drinking water represent a major health risk in developing countries (*1*) but are also a concern in developed nations (*2, 3*). In many parts of the world, carbonate (karst) aquifers are among the most important freshwater resources (*4*) but are, however, particularly vulnerable to microbial and other contamination. Contaminants can easily enter the groundwater through shallow soils or via sinking streams, and may be rapidly transported in conduit networks where attenuation processes are less effective than in other aquifer types (*5*). Karst systems often drain towards springs, which are also preferred locations of drinking water abstraction. The springs often show strong and rapid variations of discharge and water quality in response to rainfall events. Prolonged periods of good water quality may thus be interrupted by short microbial contamination events. Identifying those is a major challenge in the use of karst water sources. Bakalowicz (*6*) noted that karst aquifers are often avoided as water sources because of their vulnerability and the perceived difficulties in exploitation. Better monitoring techniques and protection strategies could help to better use these valuable resources.

Fecal indicator bacteria (FIB), particularly *E. coli* and enterococci, are widely accepted as indicators of the possible presence of pathogens (*7*). For example, good correlation was established between FIB and *Cryptosporidium* cysts in karst spring waters (*8*). However, monitoring microbial water quality relies on sterile water sampling and laboratory analyses. The sampling intervals and the time lags between sampling and results (~24 h) are often too long to prevent contaminated water entering the distribution network. An early-warning parameter would thus be of high utility for drinking water purveyors.

Suspended and dissolved matter in groundwater either comes from the aquifer itself (autochthonous) or from outside, e.g., from the land surface (allochthonous). Fecal and pathogenic bacteria often originate from agricultural activities and enter the aquifer via sinking streams or through the soil; they are thus allochthonous. In groundwater, fecal bacteria are mainly transported together with or attached to suspended particles (*9, 10*). Several authors consequently proposed turbidity as a contamination indicator (*11, 12*). However, turbidity at karst springs is a complex signal resulting from resuspension of sediments inside conduits and fractures (autochthonous) and/or transfer of particles from the soil or sinking surface streams (allochthonous) (*13*). Furthermore, small turbidity variations sometimes coincide with high FIB levels, whereas large turbidity signals can occur without microbial water contamination. Consequently, turbidity alone does not allow the identification of the origin and type of suspended particles, and is not always a reliable water quality indicator (*14*).

Total organic carbon (TOC) in groundwater mainly originates from the soil and surface waters (allochthonous) and could thus complement turbidity as an indicator for fecal contamination. However, TOC signals at karst springs often trails behind the FIB signal (*14*), whereas an ideal indicator should react simultaneously or even precede the contamination event.

Turbidity is a bulk parameter, caused by the scattering of light by suspended particles and expressed as nephelometric turbidity units (NTU), but it does not yield information about the number and size of particles. Particle counters allow particle-size distributions (PSD) to be measured online and continuously. Therefore, PSD appears to be a promising parameter to gain more insight into the origin and behavior of suspended particles in karst groundwater and, thus, a possible indicator for microbial contamination. Brookes et al. (*15*) assessed the value of PSD as surrogate indicator for pathogens in lakes and reservoirs and found good correlation between specific particle-size classes, FIB, and selected pathogens. A similar approach has been applied to marine bathing waters, where PSD measurement using a low-angle light scattering instrument revealed correlation between dinoflagellates and a specific particle-size class (*16*). The relation between PSD and FIB in karst groundwater has not yet been assessed in detail.

Atteia and coworkers studied the size distribution and chemical−mineralogical composition of colloids and particles from a sinking stream and a connected karst spring (*17, 18*). PSD curves at the spring were composed of two

* Corresponding author phone: +41 32 718 2645; fax: +41 32 718 2603; e-mail: nico.goldscheider@unine.ch.
[†] Center of Hydrogeology.
[‡] Laboratory of Microbiology.

10.1021/es071976f CCC: $37.00

Published on Web 11/09/2007

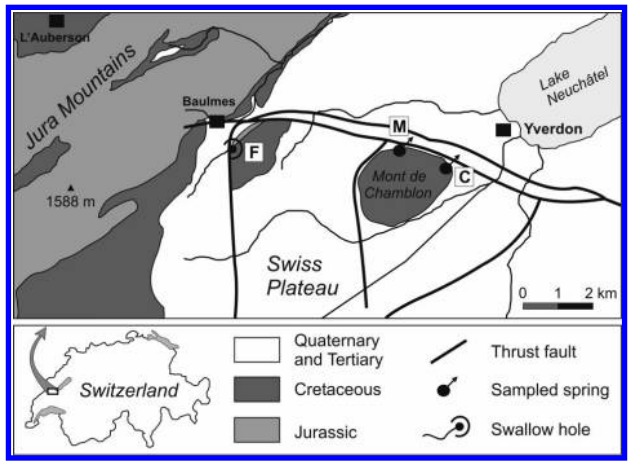

FIGURE 1. Geological map of the study area showing the locations of the swallow hole (F: Feurtille) and the karst springs (M: Moulinet, C: Cossaux) (modified after *14*).

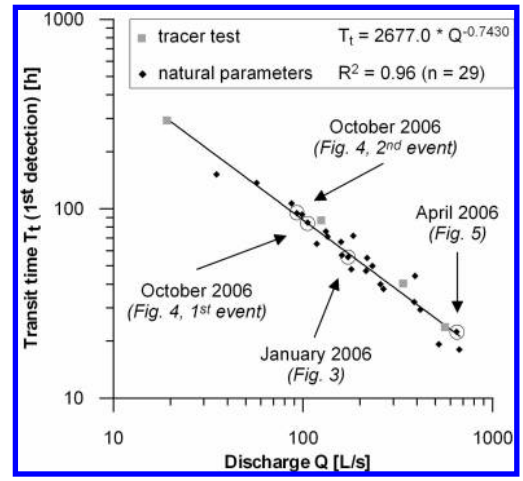

FIGURE 2. Relationship between discharge at the Moulinet spring and transit time between the swallow hole and the spring, obtained from monitoring of natural parameters after precipitation events and from tracer tests. Transit times are spans of time between the moment of discharge increase at the swallow hole (for natural parameters) or the time of injection (for artificial tracers), and the time when the respective parameter started to increase at the spring.

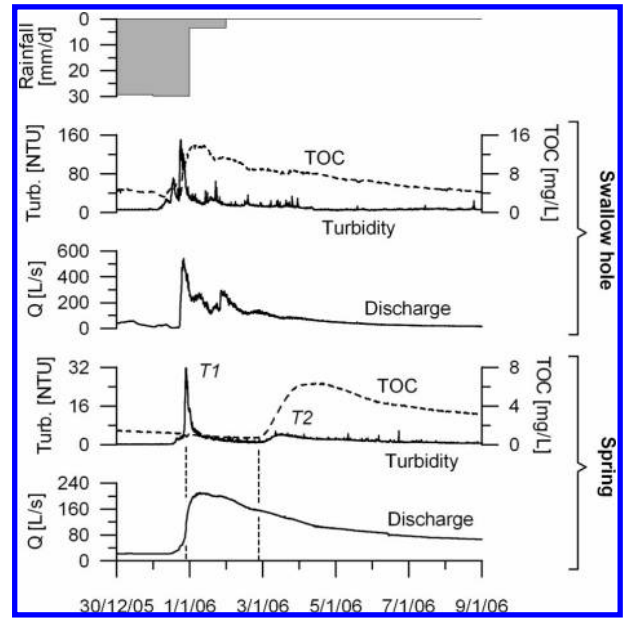

FIGURE 3. Autochthonous (T1) and allochthonous (T2) turbidity signals at the Moulinet karst spring after a heavy rainfall event, preceded and followed by dry periods (*Q* = discharge; Turb. = turbidity).

distinct parts with a break point at 4–5 μm. Smaller particles were mainly influenced by pH, whereas larger particles were closely related to discharge. The break point was consequently interpreted as the limit between colloidal and particle behavior, although the limit is typically defined at 1 μm. The study also included FIB analyses; however, sampling intervals for both PSD and FIB were too large to resolve temporal variability and establish coherences between the two groups of parameters.

The main objectives of the present study are (i) to better understand the origin, transport, and behavior of particles and fecal bacteria in karst groundwater flow systems; and (ii) to point out a surrogate parameter for possible fecal contamination that can be measured online and continuously. Two test sites in Switzerland were monitored for various physicochemical parameters, PSD, and FIB from January 2005 to June 2007. Results from the main test site near the city of Yverdon will be presented here.

Experimental Section

Study Area. The Yverdon karst aquifer system is located between two major geological units: the Jura Mountains and the Swiss Plateau (Figure 1). Karstified Jurassic−Cretaceous limestone outcrops in two hydrogeological windows within low-permeability Quaternary and Tertiary sediments (*19*). At the western hydrogeological window, a stream draining an agricultural area sinks into a swallow hole (Feurtille) at 600 m altitude. Two springs at about 450 m (Moulinet and Cossaux) discharge from the eastern window: the Moulinet spring consist of eight outlets showing identical physicochemical characteristics; the Cossaux spring is tapped by inclined drillings and contributes to regional water supply. The springs show similar temporal evolutions of physicochemical and microbiological parameters, whereas the absolute levels are different: Lower nitrate, FIB and turbidity levels and 2–3 °C higher temperatures occur at Cossaux, indicating higher contribution of cleaner and warmer groundwater from greater depth (*14, 20*). We mainly present data from Moulinet spring, because higher contamination levels make it easier to illustrate the problem. However, the results from Cossaux spring are very similar.

Four quantitative tracer tests between the swallow hole and the springs, as well as monitoring of natural parameters, made it possible to identify the swallow hole as the major source of microbial water quality deterioration, mainly after heavy rainfalls. Transit times varied from 12 days during low-flow to less than 24 hours during high-flow conditions (Figure 2). With increasing discharge, tracer recoveries increase at the Moulinet spring but decrease at the Cossaux spring, whereas total recovery remains nearly constant at ~29 %, indicating that Moulinet acts as an overflow of the Cossaux spring.

Monitoring Program and Methods. Discharge (Q), water temperature (T°), electrical conductivity (EC), turbidity (Turb.), and TOC were monitored continuously at the swallow hole and the springs. Discharge was measured by means of weirs and pressure probes (DL/N64, STS, Sirnach, Switzerland). Temperature and EC were recorded using conductivity probes (340i, WTW, Weilheim, Germany) and data loggers (DT50, DataTaker, Rowville, Australia). Turbidity and TOC were measured with submersible fluorometers (GGUN-FL30, Neuchâtel, Switzerland). The long-term stability of all instruments was controlled on-site and in the laboratory.

For long-term monitoring, water was collected in sterile bottles twice a month, transported to the laboratory in cooling

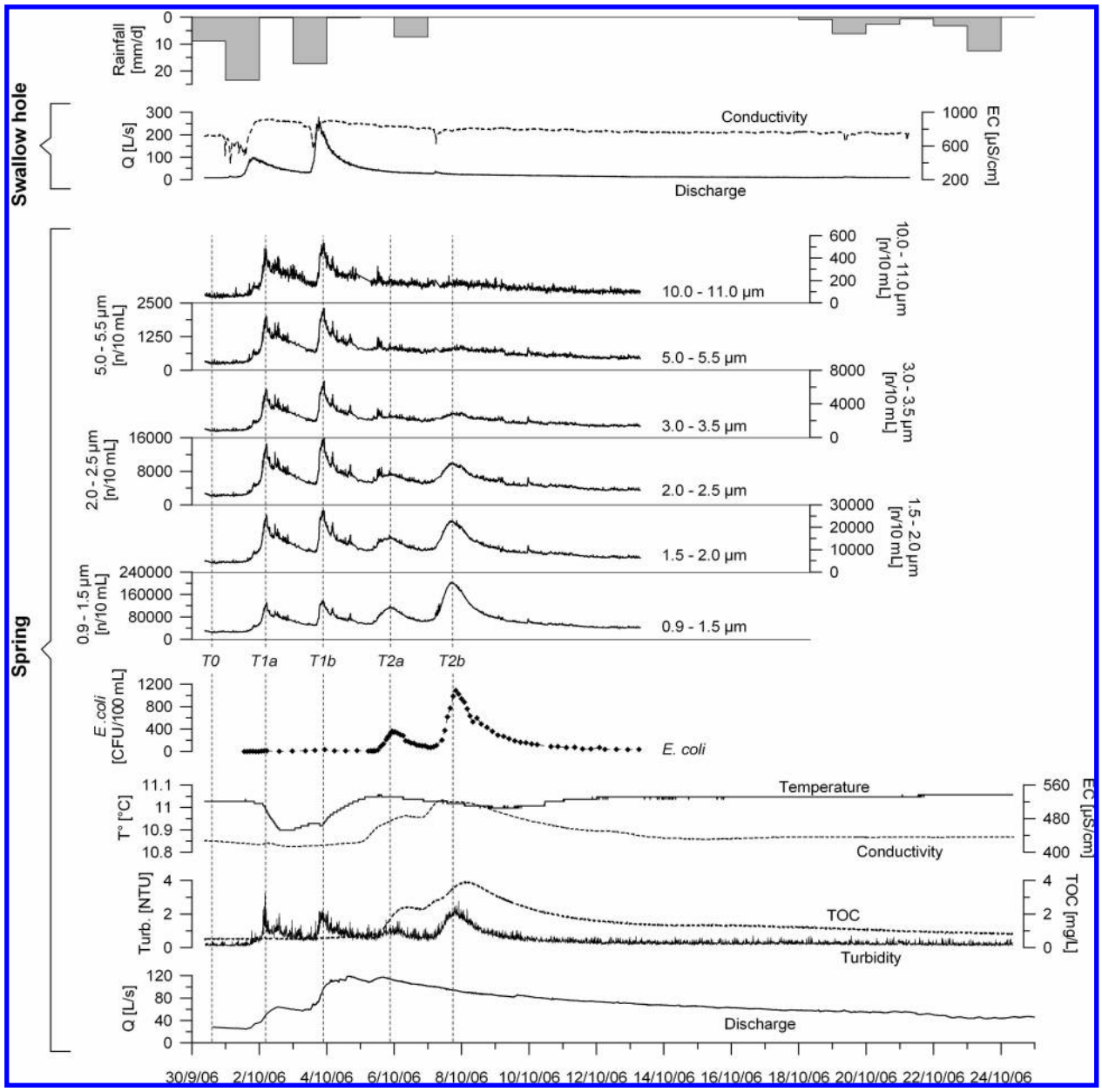

FIGURE 4. Dynamics of natural parameters during a multiple flood event at the Feurtille swallow hole and the Moulinet spring. T0: pre-storm conditions, T1a/b: autochthonous turbidity signals of the first/second flood event, T2a/b: allochthonous turbidity signals of the first/second flood event.

boxes and processed within 6 h. Samples were analyzed for PSD, major ion chemistry and FIB, including total coliforms (TC), mesophilic aerobic bacteria (MAB), enterococci and *Escherichia coli*. During selected hydrological events, PSD was monitored continuously on-site, and water samples for chemistry and FIB were taken hourly by an automatic sampler (6712C, ISCO, Lincoln, NE) in sterilized bottles. During these events, samples were processed within 6 h (for the latest sample) to 30 h (for the earliest sample). Control analyses showed that this approach did not falsify the results. PSD measurements were done with a portable particle counter (Abakus mobil fluid, Klotz, Bad Liebenzell, Germany) that counts suspended particles in the range of 0.9–139 μm and groups them into up to 32 definable size classes. Major ions were analyzed by an ion chromatograph (DX-120, Dionex, Sunnyvale, CA). Bacteria were enumerated using standard cultivation techniques (*21*).

Preliminary monitoring of a flood event revealed good correlation between *E. coli* and enterococci ($R^2 = 0.92$, $n = 77$). Furthermore, it is increasingly recognized that TC and MAB have low sanitary significance (*7*). Therefore, the high-resolution monitoring presented here focused on *E. coli*. Results are alternately single and duplicate determinations, expressed as colony forming units (CFU) per 100 mL.

Daily precipitation data (MeteoSwiss) from three stations were considered: Yverdon-les-Bains (altitude: 433 m), Baulmes (642 m), and L'Auberson (1110 m) (Figure 1). For reasons of simplicity, only the data from Baulmes are presented here.

Results and discussion

Single Flood Event. Figure 3 shows the typical response of the system to an intense rainfall event, preceded and followed by long dry periods. During this event, large quantities of suspended particles (turbidity) and TOC entered the swallow hole. The discharge of the Moulinet spring increased from 21 to 207 L/s. A first turbidity signal (T1) in the spring water occurred during the rising limb of the hydrograph, reached a maximum of 32 NTU before the discharge maximum, and then decreased down to its initial level, while TOC remained on a low level. This first turbidity signal can be attributed to

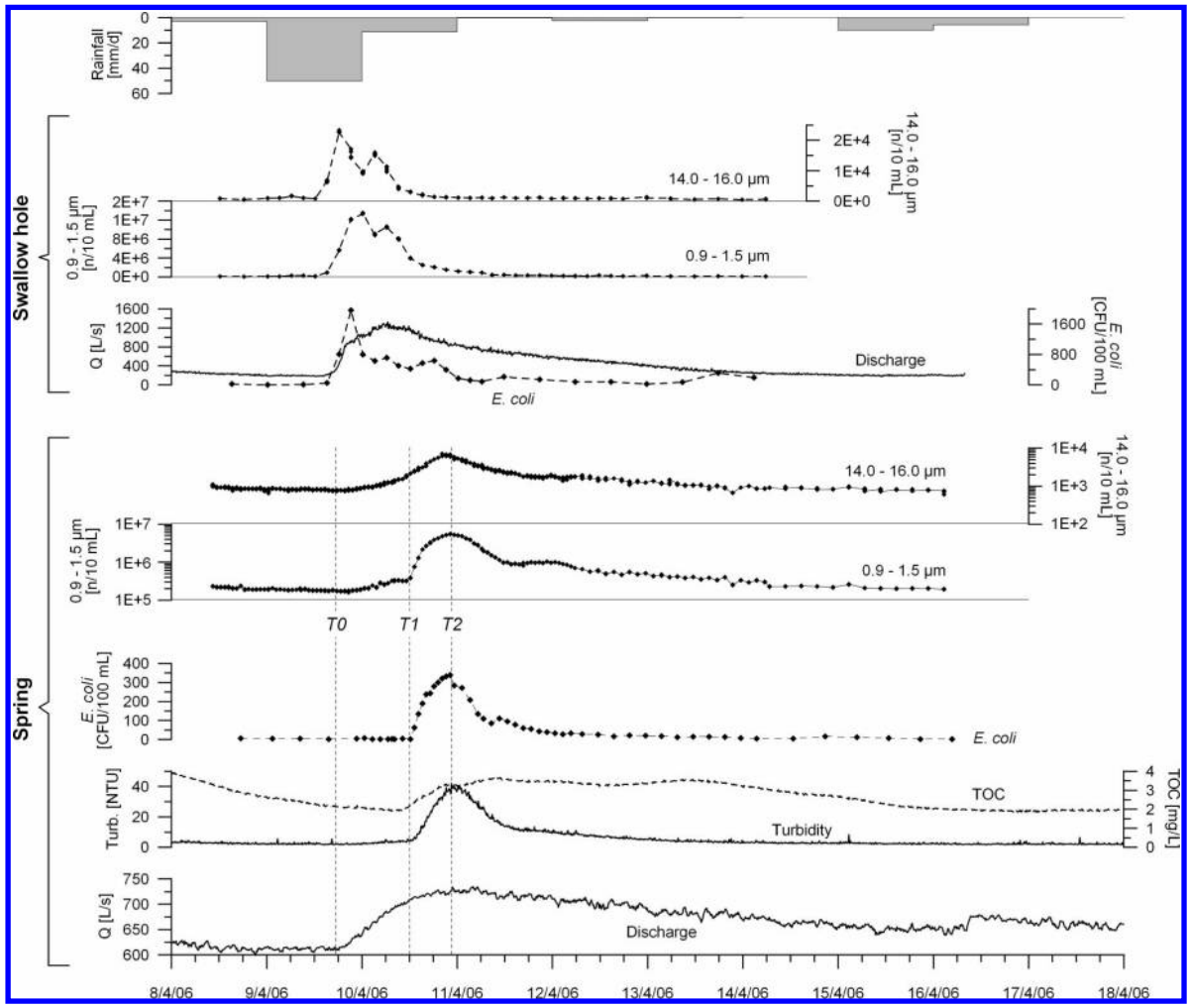

FIGURE 5. Dynamics of natural parameters during snowmelt and intense rainfall at the swallow hole and the Moulinet spring. T0: prestorm conditions, T1: maximum of exclusively autochthonous turbidity, T2: maximum of allochthonous turbidity.

the resuspension of sediments inside karst conduits, relatively near to the spring, due to increasing flow velocities and turbulences. Consequently, T1 represents autochthonous turbidity.

Two days after the rainfall, when discharge was in the recession stage, a simultaneous increase of TOC and turbidity (T2) was observed at the spring. This secondary signal can be attributed to the arrival of storm-derived water from the swallow hole and is thus of allochthonous origin. The time lag between the infiltration event and the arrival at the spring corresponds well to the discharge-dependent transit time obtained by tracer tests (Figure 2).

Both at the swallow hole and the spring, the turbidity signals precede the TOC signals and are narrower than those. This observation is consistent with the findings of studies from porous media, which revealed faster transport of colloids with respect to solutes due to exclusion processes (*22–25*). Comparative tracer tests in karst aquifers suggest that similar processes also operate there (*8, 26*). In the present case, the time lag between the turbidity and TOC maximums at the swallow hole (10 h) can be attributed to differential transport processes in the catchment of the swallow hole, whereas the longer time lag observed at the spring (24 h) indicates that suspended particles travel at higher mean velocities in karst conduits than TOC. This can be explained by exclusion (i.e. particle travel along the fastest flow lines while solutes sample the entire fluid volume) and/or a time-dependent loss function (i.e. fast particles arrive at the spring, while slow particles are removed).

The analysis of this single event makes it possible to better understand and resolve the response of the aquifer system on more complex conditions, such as multiple rainfall events or rainfall and snowmelt.

Multiple Flood Event. Two shortly successive rainfall events were monitored in Autumn 2006 (Figure 4). The discharge of the sinking stream shows two peaks: it increased from 7 to 97 L/s on October 1 and from 30 to 280 L/s on October 3, followed by rapid recession. High levels of turbidity (90 NTU), TOC (14 mg/L) and FIB (>3000 CFU/100 mL) entered the swallow hole (data not shown). The discharge of the Moulinet spring increased almost immediately in response to the rainfall events from 26 L/s to a first maximum of 63 L/s and a second maximum of 119 L/s. During the rising limbs of these discharge pulses, turbidity displayed two distinct peaks (T1a/b) of ~2 NTU, while *E. coli*, TOC and EC remained at their low pre-storm levels. These turbidity signals thus result from the remobilization of autochthonous sediments inside karst conduits due to increasing flow rates.

In the following days, when the spring was in a recession period, two successive increases of turbidity (T2a/b), TOC, EC and *E. coli* were monitored. Turbidity reached 1 and 2.5 NTU, respectively, while *E. coli* first increased from 0 to 362 and then to 1088 CFU/100 mL. This behavior can only be attributed to the arrival of turbid and contaminated water from the sinking stream that infiltrated during the two rainfall events (allochthonous). The time lags between the two discharge increases at the swallow hole and the corresponding arrivals at the spring are 95 and 85 h, respectively, which falls

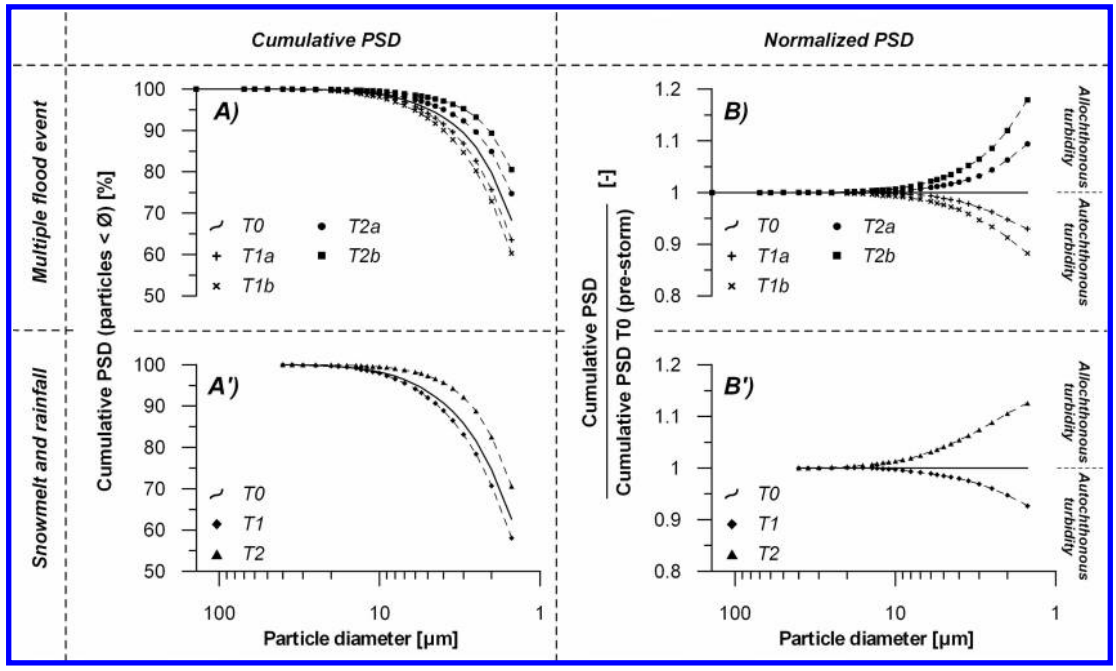

FIGURE 6. Analysis of selected PSD curves (sampling times *T* are shown in Figures 4 and 5). A relative increase of finer particles (0.9–10 μm) with respect to a pre-storm reference PSD is indicative of allochthonous turbidity and, thus, the possible presence of fecal bacteria contamination.

in the range of the tracer results (Figure 2). The higher mean discharge during the second phase explains the shorter transit time.

The particle counter yields more detailed analyses of the turbidity signals and their origin: The two primary, autochthonous signals (T1a/b) were caused by simultaneous increases of all particle-size classes, including diameters >5 μm. During the two secondary, allochthonous signals (T2a/b), only smaller particles (0.9–5.0 μm) increased, while larger particles were in a recession period. During the allochthonous turbidity period, finer particles and *E. coli* display a nearly perfectly parallel evolution and, thus, a high correlation (R^2 = 0.93). The flow-pulses following intense rainfall thus remobilize particles of a wide range of diameters from karst conduits near the spring, while only small particles are transported along the entire pathway from the sinking stream to the spring, along with fecal bacteria.

At the Cossaux spring, all parameters evolved similarly, but at lower levels. The maximums of turbidity (0.9 NTU) and TOC (0.9 mg/L) did not exceed the water quality standards of 1 NTU and 1 mg/L, respectively, whereas *E. coli* reached two distinct maximum levels of 116 and 383 CFU/100 mL during phases T2a and T2b, respectively. PSD, however, showed clear maximums of the finer particle-size classes during these two contamination events.

Snowmelt and Rainfall. The combined influence of snowmelt and storm rainfall was monitored in spring 2006 (Figure 5). Snowmelt caused a high and relatively stable flow rate of ~610 L/s at the spring, causing short transit times between the swallow hole and the spring, about 22 hours (Figure 2). *E. coli* and turbidity levels were very low and stable, and TOC was in a slow recession phase.

A storm rainfall occurred on April 9–10. The discharge of the sinking stream showed a sharp increase from 200 to 1200 L/s, associated with high levels of *E. coli* (up to 2000 CFU/100 mL), TOC (10 mg/L), nitrate (43 mg/L) and turbidity (>150 NTU). The turbidity entering the swallow hole is composed of a wide range of particle-sizes, but the larger particles peaked before the smaller ones, which can be explained by their different origins: large particles mainly result from erosion in the stream channel and at the soil surface, while smaller particles (colloids) come from percolation through the soil towards a network of artificial drainage tubes. In terms of both absolute and relative quantity, smaller particles dominate the input at the swallow hole. At the moment of maximum turbidity, the concentration of 0.9–1.5 μm particles was 170 times the prestorm value, against 19 times for 14.0–16.0 μm particles.

During the rising limb of the spring hydrograph (T0−T1 in Figure 5), turbidity increased from 2 to 5 NTU, whereas TOC was still decreasing and *E. coli* was constantly low at 0–1 CFU/100 mL. This corresponds to a typical autochthonous signal. About 22 hours after the first response of the spring, all parameters displayed a sudden increase, with maximum *E. coli* levels of 340 CFU/100 mL and a turbidity maximum of 40 NTU (T2), clearly originating from the swallow hole (allochthonous).

During the first phase, all particle-size classes showed a similar evolution and increased steadily. In Figure 5, only two size classes are shown, representative for fine (0.9–1.5 μm) and large particles (14–16 μm). From the moment when the water from the swallow hole first arrived (T1), the different particle-size classes evolve differently: larger particles continue to increase steadily, whereas smaller particles display an abrupt break point and sharp increase, which coincides with the arrival and evolution of *E. coli*. The larger particles can mainly be attributed to resuspension of sediments from karst conduits near the spring, whereas the finer particles originate from the swallow hole. The autochthonous and allochthonous turbidity signals thus superimpose during this flood, but PSD analyses make it possible to differentiate the two signals and recognize the turbidity that brings fecal contamination.

Normalized PSD as Surrogate Indicator for Microbial Contamination. The results presented above show that FIB contamination occurs during allochthonous turbidity events, whereas autochthonous turbidity is hygienically safe. In the simplest case, when there are two clearly discernible turbidity signals, the second one indicates the arrival of fecal bacteria, although low turbidity levels sometimes coincide with high bacteria levels and vice versa. In more complex cases, however, turbidity signals may overlap, and PSD analyses

are required to discriminate the two signals and better identify contamination periods. As shown above, autochthonous turbidity consists of a wide range of particle sizes, including larger particles, whereas allochthonous turbidity and bacterial contamination periods are characterized by predominance of finer particles. However, in absolute numbers, finer particles are always more abundant than larger ones. It is thus necessary to achieve a more advanced analysis of PSD.

As a first step, PSD curves are presented in a cumulative form, i.e., percent of particles smaller than a given diameter vs. particle diameter (Figure 6 A and A′). In this presentation, the PSD curves of the prestorm conditions are plotted as reference curves (T0). The PSD of autochthonous turbidity events (T1) lie below this reference curve, whereas the PSD of allochthonous turbidity periods (T2) lie above, indicating a relative predominance of finer particles. The difference becomes even more evident when all PSD curves are normalized by the reference PSD (Figure 6 B and B′). In this presentation, the reference PSD is a horizontal line ($Y = 1$), while finer particle-classes display values <1 for autochthonous turbidity and >1 for allochthonous turbidity.

Recent unpublished findings from the Noiraigue karst spring and its catchment in the Swiss Jura Mountains, partly based on earlier studies (*17, 18*), confirm the feasibility of this approach. Compared to the Yverdon area, this site is located at higher altitudes, the land use is different, the unsaturated zone is thicker, the aquifer is recharged by several swallow holes and diffuse infiltration through the soil, and the spring reacts faster and stronger to rainfall. Correspondingly, the turbidity, TOC and FIB signals are different and more complex. However, also in this case, PSD analyses made it possible to discriminate the different types of turbidity and to identify microbial contamination periods.

As a conclusion, PSD monitoring of karst spring waters makes it possible to distinguish between turbidity resulting from the resuspension of sediments inside the aquifer and turbidity derived from the land surface. The second type often coincides with increased levels of microbial contamination originating from agricultural and other activities at the land surface. Continuous PSD monitoring can thus be used as an early-warning system for fecal contamination of spring water. The method is applicable for aquifer systems with different hydrogeological settings, although local adaptations may be required. For example, there is no universal and absolute relation between PSD and fecal bacteria, but this relation depends on the type and intensity of land use and on the aquifer properties. The method can be simplified and automated by using particle counters with only few size classes, and by continuous data evaluation. This information can be used to optimize the water treatment or disconnect the spring from the distribution network during contamination periods, whereas the spring water could still be used in periods when the water contains increased levels of turbidity but is hygienically safe.

Acknowledgments

We thank the water supply company of Yverdon-les-Bains (SEY) for cooperation, technical, and logistic support, and the Swiss National Science Foundation (grant no. 200020-113609/1) for funding.

Literature Cited

(1) Montgomery, M. A.; Elimelech, M. Water and sanitation in developing countries: Including health in the equation. *Environ. Sci. Technol.* **2007**, *41*, 17–24.
(2) Herwaldt, B. L.; Craun, G. F.; Stokes, S. L.; Juranek, D. D. Outbreaks of waterborne disease in the United-States - 1989–90. *J. Am. Water Work Assoc.* **1992**, *84*, 129–135.
(3) Rose, J. B.; Gerba, C. P.; Jakubowski, W. Survey of potable water-supplies for *Cryptosporidium* and *Giardia*. *Environ. Sci. Technol.* **1991**, *25*, 1393–1400.
(4) Ford, D.; Williams, P. *Karst Hydrogeology and Geomorphology*; Wiley: New York, 2007.
(5) Drew, D.; Hötzl, H. Karst Hydrogeology and Human Activities. *Impacts, Consequences and Implications*. International Contributions to Hydrogeology (IAH); Balkema: Rotterdam, Brookfield, 1999.
(6) Bakalowicz, M. Karst groundwater: a challenge for new resources. *Hydrogeol. J.* **2005**, *13*, 148–160.
(7) Doyle, M. P.; Erickson, M. C. Closing the door on fecal coliform assay. *Microbe* **2006**, *1*, 162–163.
(8) Auckenthaler, A.; Raso, G.; Huggenberger, P. Particle transport in a karst aquifer: natural and artificial tracer experiments with bacteria, bacteriophages and microspheres. *Water Sci. Technol.* **2002**, *46*, 131–138.
(9) Mahler, B. J.; Personne, J. C.; Lods, G. F.; Drogue, C. Transport of free and particulate-associated bacteria in karst. *J. Hydrol.* **2000**, *238*, 179–193.
(10) Hipsey, M. R.; Brookes, J. D.; Regel, R. H.; Antenucci, J. P.; Burch, M. D. In situ evidence for the association of total coliforms and *Escherichia coli* with suspended inorganic particles in an Australian reservoir. *Water, Air, Soil Pollut.* **2006**, *170*, 191–209.
(11) Nebbache, S.; Loquet, M.; Vinceslas-Akpa, M.; Feeny, V. Turbidity and microorganisms in a karst spring. *Eur. J. Soil Biol.* **1997**, *33*, 89–103.
(12) Ryan, M.; Meiman, J. An examination of short-term variations in water quality at a karst spring in Kentucky. *Ground Water* **1996**, *34*, 23–30.
(13) Massei, N.; Wang, H. Q.; Dupont, J. P.; Rodet, J.; Laignel, B. Assessment of direct transfer and resuspension of particles during turbid floods at a karstic spring. *J. Hydrol.* **2003**, *275*, 109–121.
(14) Pronk, M.; Goldscheider, N.; Zopfi, J. Dynamics and interaction of organic carbon, turbidity and bacteria in a karst aquifer system. *Hydrogeol. J.* **2006**, *14*, 473–484.
(15) Brookes, J. D.; Hipsey, M. R.; Burch, M. D.; Regel, R. H.; Linden, L. G.; Ferguson, C. M.; Antenucci, J. P. Relative value of surrogate indicators for detecting pathogens in lakes and reservoirs. *Environ. Sci. Technol.* **2005**, *39*, 8614–8621.
(16) Ahn, J. H.; Grant, S. B. Size distribution, sources, and seasonality of suspended particles in southern California marine bathing waters. *Environ. Sci. Technol.* **2007**, *41*, 695–702.
(17) Atteia, O.; Kozel, R. Particle size distributions in waters from a karstic aquifer: from particles to colloids. *J. Hydrol.* **1997**, *201*, 102–119.
(18) Atteia, O.; Perret, D.; Adatte, T.; Kozel, R.; Rossi, P. Characterization of natural colloids from a river and spring in a karstic basin. *Environ. Geol.* **1998**, *34*, 257–269.
(19) Burkhard, M.; Atteia, O.; Sommaruga, A.; Gogniat, S.; Evard, D. Tectonics and hydrogeology of the Neuchatel Jura. *Eclogae Geol. Helv.* **1998**, *91*, 177–183.
(20) Muralt, R.; Vuataz, F. D.; Schonborn, G.; Sommaruga, A.; Jenny, J. Integration of hydrochemical, geological and geophysical methods for the exploration of a new thermal water resource. Case of Yverdon-les-Bains, foot of the Jura range. *Eclogae Geol. Helv.* **1997**, *90*, 179–197.
(21) APHA; AWWA, *WEF Standard Methods for the Examination of Water and Wastewater*, 21st Edition; Water Environment Federation: Alexandria, VA, 2005.
(22) Bradford, S. A.; Simunek, J.; Bettahar, M.; Van Genuchten, M. T.; Yates, S. R. Modeling colloid attachment, straining, and exclusion in saturated porous media. *Environ. Sci. Technol.* **2003**, *37*, 2242–2250.
(23) Sirivithayapakorn, S.; Keller, A. Transport of colloids in saturated porous media: A pore-scale observation of the size exclusion effect and colloid acceleration. *Water Resour. Res.* **2003**, *39*.
(24) Keller, A. A.; Sirivithayapakorn, S.; Chrysikopoulos, C. V. Early breakthrough of colloids and bacteriophage MS2 in a water-saturated sand column. *Water Resour. Res*, **2004**, *40*.
(25) Grolimund, D.; Elimelech, M.; Borkovec, M.; Barmettler, K.; Kretzschmar, R.; Sticher, H. Transport of in situ mobilized colloidal particles in packed soil columns. *Environ. Sci. Technol.* **1998**, *32*, 3562–3569.
(26) Göppert, N.; Goldscheider, N. Solute and colloid transport in karst conduits under low and high flow conditions. *Ground Water*,published online. DOI: 10.1111/j.1745-6584.2007.00373.x.

ES071976F